

Tapered gradient-index media and zone plates: influence of off-axis illumination and finite dimension on light propagation

JOSÉ MANUEL RIVAS-MOSCOSO, CARLOS GÓMEZ-REINO,

MARÍA VICTORIA PÉREZ and CARMEN BAO

Laboratorio de Óptica, Departamento de Física Aplicada, Escola de Óptica e
Optometría and Facultade de Física, Universidade de Santiago de Compostela,
E15706 Santiago de Compostela, Galicia, Spain

phone/fax: +34981521984

e-mail: facgrc@usc.es

Abstract. The effects of off-axis illumination and finite dimension on the irradiance distribution in a hybrid system formed by a zone plate and a tapered gradient-index (GRIN) medium are investigated. Results are applied to a GRIN medium with a divergent linear taper function and a sinusoidal zone plate of amplitude to show the transverse shift and the diffractive effect.

Keywords: GRIN optics, zone plates, finite-aperture diffractive effect, image formation.

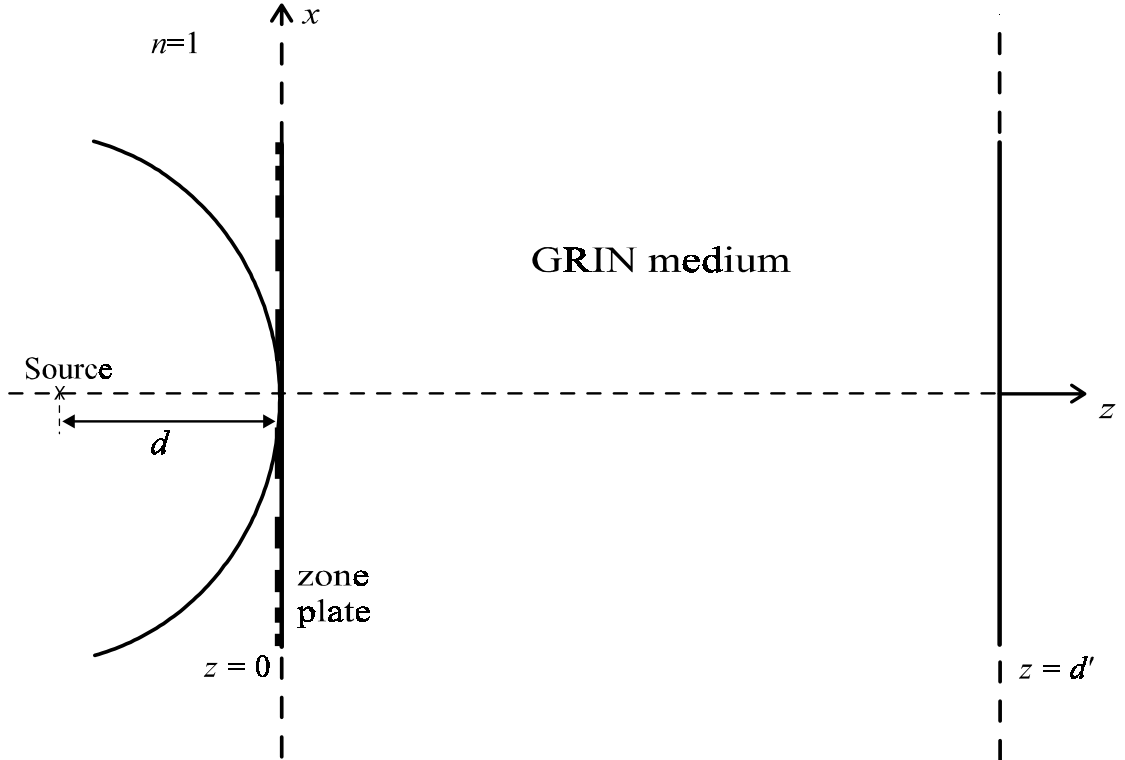


Figure 1: Geometry for the evaluation of the complex amplitude distribution in a hybrid optical system, tapered GRIN medium/zone plate, illuminated by a cylindrical uniform wavefront. Parameter d represents the distance from the point source to the zone plate.

1 Introduction

Recently, the authors have studied light propagation through a hybrid optical system formed by a zone plate and a tapered gradient-index (GRIN) medium [1]. In this paper, theoretical aspects of the light propagation were investigated assuming strictly hybrid systems of infinite dimensions illuminated by coherent non-uniform and uniform beams. In particular, imaging and transforming phenomena as well as an analogy with an apparent lens of multifocal distance were derived and discussed. Such a theoretical description is sufficient for many studies. However, it is important to realize the effects arising as a result of the departure from the theoretical model. In this way, the aim of this paper is to study the influence of the lateral displacement of the source and of the finite transverse dimension of the hybrid system as a logical continuation of the previous work. This optical system could have possible applications in imaging and transforming of periodic objects, integrated optics for transverse couplers [2, 3, 4], etc.

The study will be restricted to the one-dimensional transverse case, but extension to the two-dimensional case is straightforward.

The plan of the paper is as follows. In section 2 we obtain the irradiance in an infinite hybrid system tapered GRIN medium/zone plate. In sections 3 and 4 the effects on the irradiance distribution which arise as a result of off-axis illumination and of the finite dimension of the hybrid system are studied and analysed. Conclusions are presented in section 5.

2 Irradiance distribution in a tapered GRIN medium for an infinite zone plate and uniform illumination

Let us consider a tapered GRIN planar medium characterized by a transverse parabolic refractive index modulated by an axial taper function and whose refractive index profile is given by

$$n^2(x, z) = n_0^2 [1 - g^2(z)x^2], \quad (1)$$

where n_0 is the index at the z optical axis and $g(z)$ the taper function that describes the evolution of the transverse index along the z axis.

We assume a one-dimensional zone plate of infinite dimension located at the input of the GRIN medium and whose transmission function will be represented as

$$T(x_0) = \sum_{m=-\infty}^{+\infty} a_m \exp \left\{ -i \frac{2\pi m}{p} x_0^2 \right\}, \quad (2)$$

where p is the spatial period and a_m the amplitude of the m th harmonic.

When the hybrid optical system formed by the zone plate and the tapered GRIN medium is illuminated by a coherent uniform beam (figure 1), the complex amplitude distribution on the zone plate located at $z = 0$ can be written as

$$\phi(x_0) = T(x_0) \psi_0(x_0), \quad (3)$$

where

$$\psi_0(x_0) = \frac{\exp(ikd)}{d^{1/2}} \exp \left\{ i \frac{\pi}{\lambda d} x_0^2 \right\} \quad (4)$$

is the complex amplitude distribution due to a cylindrical wavefront of wavelength λ and curvature radius d .

The complex amplitude distribution in the tapered GRIN medium at $z > 0$ is given by the integral equation [1]

$$\phi(x; z) = \int_{-\infty}^{\infty} \phi(x_0) K(x, x_0; z) dx_0, \quad (5)$$

$K(x, x_0; z)$ being the one-dimensional optical propagator of this medium expressed as

$$K(x, x_0; z) = \left[\frac{n_0}{i\lambda H_1(z)} \right]^{1/2} \exp \{ i k n_0 z \} \exp \left\{ i \frac{k n_0}{2 H_1(z)} \left[x^2 \dot{H}_1(z) + x_0^2 H_2(z) - 2 x x_0 \right] \right\}, \quad (6)$$

where $H_1(z)$, $H_2(z)$, $\dot{H}_1(z)$ and $\dot{H}_2(z)$ are the position and the slope of the axial and field rays at z , respectively:

$$H_1(z) = [g_0 g(z)]^{-1/2} \sin \left[\int_0^z g(z') dz' \right] = - [g_0 g(z)]^{-1} \dot{H}_2(z), \quad (7)$$

$$H_2(z) = \left[\frac{g_0}{g(z)} \right]^{1/2} \cos \left[\int_0^z g(z') dz' \right] = \frac{g_0}{g(z)} \dot{H}_1, \quad (8)$$

the dot being the derivative with respect to z and g_0 the value of $g(z)$ at $z = 0$.

Substituting equations (2)-(4) and (6) into equation (5) we have

$$\begin{aligned} \phi(x; z) &= \left(\frac{n_0}{i\lambda d H_1(z)} \right)^{1/2} \exp \{ ik(n_0 z + d) \} \\ &\times \exp \left\{ i \frac{kn_0}{2H_1(z)} \dot{H}_1(z) x^2 \right\} \sum_{m=-\infty}^{\infty} a_m \int_{-\infty}^{\infty} \exp \left\{ i \frac{\pi}{\lambda} \left(\frac{1}{d} - \frac{2m\lambda}{p} \right) x_0^2 \right\} \\ &\times \exp \left\{ i \frac{kn_0}{2H_1(z)} [H_2(z) x_0^2 - 2xx_0] \right\} dx_0. \end{aligned} \quad (9)$$

By integration, equation (9) becomes

$$\phi(x; z) = \frac{1}{d^{1/2}} \exp \{ ik(n_0 z + d) \} \sum_{m=-\infty}^{\infty} a'_m(z) \exp \left\{ i \frac{\pi}{\lambda} U_m(z) x^2 \right\}. \quad (10)$$

In equation (10) the amplitude $a'_m(z)$ and the complex curvature $U_m(z)$ of the m th diffraction order are given by

$$a'_m(z) = \frac{a_m}{F_m^{1/2}(z)}, \quad (11)$$

$$U_m(z) = n_0 \frac{d}{dz} \ln F_m(z) = n_0 \dot{F}_m(z) F_m^{-1}(z), \quad (12)$$

where

$$F_m^{(\cdot)}(z) = \left(\frac{1}{d} - \frac{2m\lambda}{p} \right) \frac{\dot{H}_1(z)}{n_0} + \dot{H}_2(z). \quad (13)$$

From equation (10) it follows that the irradiance distribution along the GRIN medium can be written as

$$I(x; z) = \frac{1}{d} \sum_{m,l=-\infty}^{\infty} a'_m(z) a_l'^*(z) \exp \left\{ i \frac{\pi}{\lambda} [U_m(z) - U_l(z)] x^2 \right\}. \quad (14)$$

Let us particularize the study to the case of a hybrid optical structure formed by a sinusoidal zone plate of amplitude and a planar GRIN medium with a divergent taper function.

The divergent linear taper function of the planar GRIN medium is given by [1, 5]

$$g(z) = \frac{g_0}{1 + z/L}, \quad (15)$$

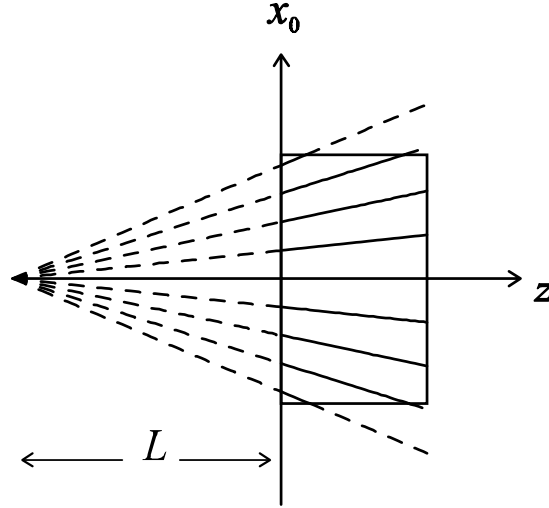


Figure 2: Equi-index lines for a divergent linear tapered GRIN medium.

L being the distance from $z = 0$ to the common apex of the equi-index lines (figure 2).

The transmission function of the sinusoidal zone plate of amplitude is expressed as [6]

$$T_s^a(x_0) = \frac{1}{2} + \frac{\varepsilon}{4i} \exp \left\{ i \frac{2\pi x_0^2}{p} \right\} - \frac{\varepsilon}{4i} \exp \left\{ -i \frac{2\pi x_0^2}{p} \right\}, \quad (16)$$

where ε is the peak-to-trough amplitude of the transmission function (figure 3).

In this case, the irradiance in the GRIN medium can be written as:

$$\begin{aligned} I_s^a(x; z) = & \frac{1}{4d} \left\{ \frac{1}{|F(z)|} + \frac{\varepsilon^2}{4|F_1(z)|} + \frac{\varepsilon^2}{4|F_{-1}(z)|} \right. \\ & + \frac{\varepsilon}{|F^{1/2}(z)F_1^{1/2}(z)|} \sin \left[\frac{\pi}{\lambda} [U(z) - U_1(z)] x^2 \right] \\ & + \frac{\varepsilon}{|F^{1/2}(z)F_{-1}^{1/2}(z)|} \sin \left[\frac{\pi}{\lambda} [U_{-1}(z) - U(z)] x^2 \right] \\ & \left. - \frac{\varepsilon^2}{2|F_1^{1/2}(z)F_{-1}^{1/2}(z)|} \cos \left[\frac{\pi}{\lambda} [U_{-1}(z) - U_1(z)] x^2 \right] \right\}. \quad (17) \end{aligned}$$

At planes $z = z_q$, where q is an integer, such that $H_1(z_q) = 0$, the imaging condition is verified and equation (10) reduces to

$$\phi(x; z_q) = \frac{\exp \{ ik(n_0 z - d) \}}{[H_2(z) d]^{1/2}} \exp \left\{ i \frac{\pi}{\lambda} \frac{x^2}{d H_2^2(z_q)} \right\} \sum_{m=-\infty}^{\infty} a_m \exp \left\{ -i \frac{2\pi m}{p(z_q)} x^2 \right\}, \quad (18)$$

where the spatial period of the zone plate at z_q reaches the value:

$$p(z_q) = p H_2^2(z_q), \quad (19)$$

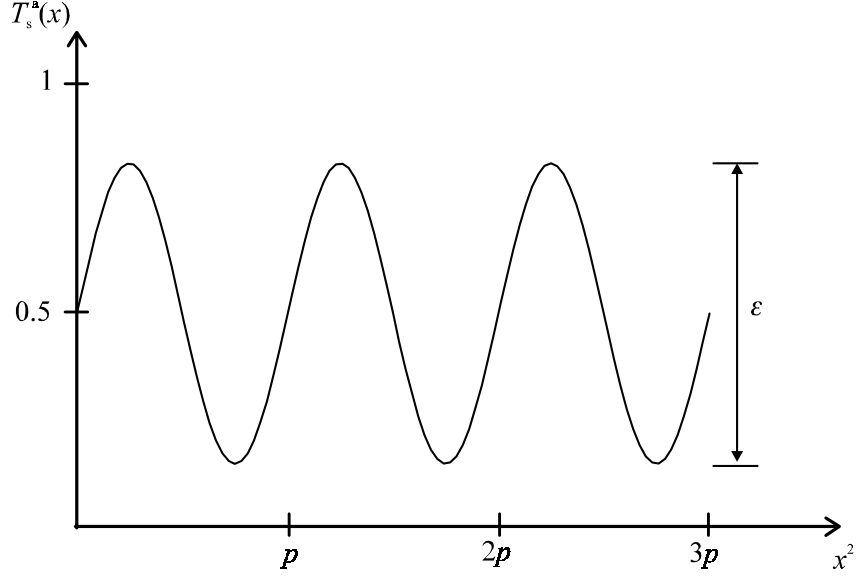


Figure 3: Transmission function of a sinusoidal zone plate of amplitude.

and the irradiance takes the form

$$I(x; z_q) = \frac{1}{d |H_2(z_q)|} \sum_{m,l=-\infty}^{\infty} a_m a_l^* \exp \left\{ -i \frac{2\pi(m-l)}{p(z_q)} x^2 \right\}. \quad (20)$$

This last equation, for the sinusoidal zone plate of amplitude, becomes

$$I_s^a(x; z_q) = \frac{1}{2d |H_2(z_q)|} \left[\frac{1}{2} + \varepsilon \sin \left(\frac{2\pi x^2}{p(z_q)} \right) + \frac{\varepsilon^2}{2} \sin^2 \left(\frac{2\pi x^2}{p(z_q)} \right) \right]. \quad (21)$$

Note the spreading of the irradiance pattern and the diminution of its contrast from an image plane to the following produced as a consequence of the divergent taper function of the medium.

3 Irradiance distribution for off-axis illumination

We suppose now an off-axis source located at a point ζ in the transverse direction from the z axis. The complex amplitude distribution on the zone plate is given by

$$\psi_0(x_0) = \frac{\exp(ikd)}{d^{1/2}} \exp \left\{ i \frac{\pi(x_0 - \zeta)^2}{\lambda d} \right\} T(x_0). \quad (22)$$

Substitution of equation (22) into equation (5) and integration provides

$$\begin{aligned} \phi(x; z) &= \frac{\exp\{ik(n_0 z + d)\}}{d^{1/2}} \sum_{m=-\infty}^{\infty} a'_m(z) \exp \left\{ i \frac{\pi}{\lambda} \left[\frac{1}{d} - \frac{H_1(z)}{n_0 F_m(z) d^2} \right] \zeta^2 \right\} \\ &\times \exp \left\{ i \frac{\pi}{\lambda} U_m(z) x^2 \right\} \exp \left\{ -i \frac{2\pi}{\lambda} \frac{\zeta x}{F_m(z) d} \right\}. \end{aligned} \quad (23)$$

From equation (23) it follows that the irradiance at a transversal plane z can be written as

$$I(x; z) = \frac{1}{d} \sum_{m,l=-\infty}^{\infty} a'_m(z) a_l'^*(z) \exp \left\{ i \frac{\pi}{\lambda} [U_m(z) - U_l(z)] x^2 \right\} \\ \times \exp \left\{ i \frac{\pi}{\lambda d} \left[\left(\frac{H_1(z) \zeta^2}{n_0 d} + 2\zeta x \right) \left(\frac{1}{F_l(z)} - \frac{1}{F_m(z)} \right) \right] \right\}. \quad (24)$$

In order to analyse the effects arising from the displacement of the source, we consider the above described hybrid system with a sinusoidal zone plate at the input. For this case, equation (24) becomes

$$I_s^a(x; z) = \frac{1}{4d} \left[\frac{1}{|F(z)|} + \frac{\varepsilon^2}{4|F_1(z)|} + \frac{\varepsilon^2}{4|F_{-1}(z)|} + \frac{\varepsilon}{|F^{1/2}(z)F_1^{1/2}(z)|} \right] \\ \times \sin \left\{ \frac{\pi}{\lambda} \left[\left(\frac{H_1(z) \zeta^2}{n_0 d^2} + \frac{2\zeta x}{d} \right) \left(\frac{1}{F_1(z)} - \frac{1}{F(z)} \right) + (U(z) - U_1(z)) x^2 \right] \right\} \\ + \frac{\varepsilon}{|F^{1/2}(z)F_{-1}^{1/2}(z)|} \sin \left\{ \frac{\pi}{\lambda} \left[\left(\frac{H_1(z) \zeta^2}{n_0 d^2} + \frac{2\zeta x}{d} \right) \left(\frac{1}{F(z)} - \frac{1}{F_{-1}(z)} \right) \right. \right. \\ \left. \left. + (U_{-1}(z) - U(z)) x^2 \right] \right\} - \frac{\varepsilon^2}{2|F_1^{1/2}(z)F_{-1}^{1/2}(z)|} \\ \times \cos \left\{ \frac{\pi}{\lambda} \left[\left(\frac{H_1(z) \zeta^2}{n_0 d^2} + \frac{2\zeta x}{d} \right) \left(\frac{1}{F_1(z)} - \frac{1}{F_{-1}(z)} \right) \right. \right. \\ \left. \left. + (U_{-1}(z) - U_1(z)) x^2 \right] \right\}. \quad (25)$$

From equations (17) and (25) it follows that an example of the difference in behaviour between on-axis and off-axis illuminations concerns the lateral shift of the irradiance pattern, since this pattern is now centred along a geometrical trajectory proportional to the axial ray which is given by

$$x_c(z) = -\dot{x}_0 H_1(z), \quad (26)$$

where $\dot{x}_0 = \zeta / (n_0 d)$ is the slope of the refracted ray at the input.

For the imaging condition, the amplitude distribution reduces to

$$\phi(x; z_q) = \frac{\exp \{ i k (n_0 z_q + d) \}}{[d H_2(z_q)]^{1/2}} \exp \left\{ i \frac{\pi}{\lambda} \frac{(x - \zeta H_2(z_q))^2}{d H_2^2(z_q)} \right\} \sum_{m=-\infty}^{\infty} a_m \exp \left\{ -i \frac{2\pi m}{p(z_q)} x^2 \right\}, \quad (27)$$

which is identical to that for on-axis illumination, given by equation (18), except for a global phase factor. Therefore, at planes $z = z_q$ the irradiance distribution remains the same whatever the transversal displacement ζ of the illumination source, and equation (26) is always zero since the axial ray $H_1(z)$ cuts the axis when the imaging condition is verified.

Figure 4 depicts the evolution of the centre of the irradiance pattern through the GRIN medium. Figure 5 shows, for comparison, the irradiance distribution at the input (a), at the plane $z = 8.5$ mm (b) and at the two first Fourier planes for off-axis (dot line) and on-axis (solid line) illuminations. Maximum lateral shifts in reverse sense are observed for these two consecutive Fourier planes ((c) and (d)). Calculations have been made in all cases for a lateral displacement $\zeta = 0.15$ mm.

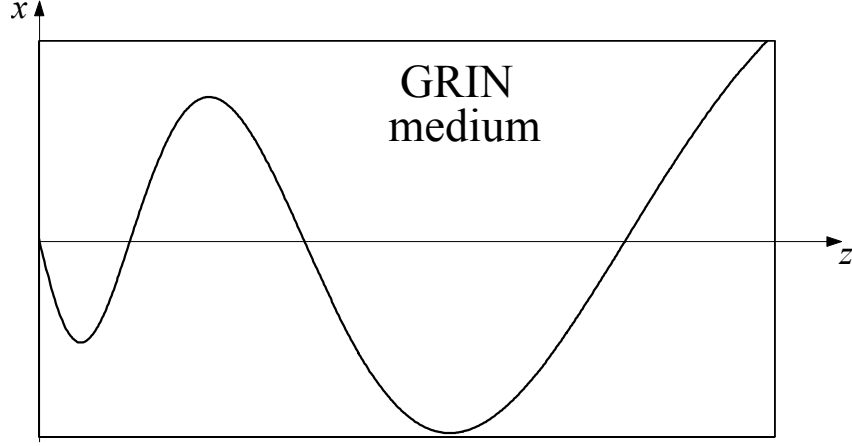


Figure 4: Geometrical trajectory described by the centre of irradiance pattern. Trajectory amplitude is increasing due to divergent linear taper function.

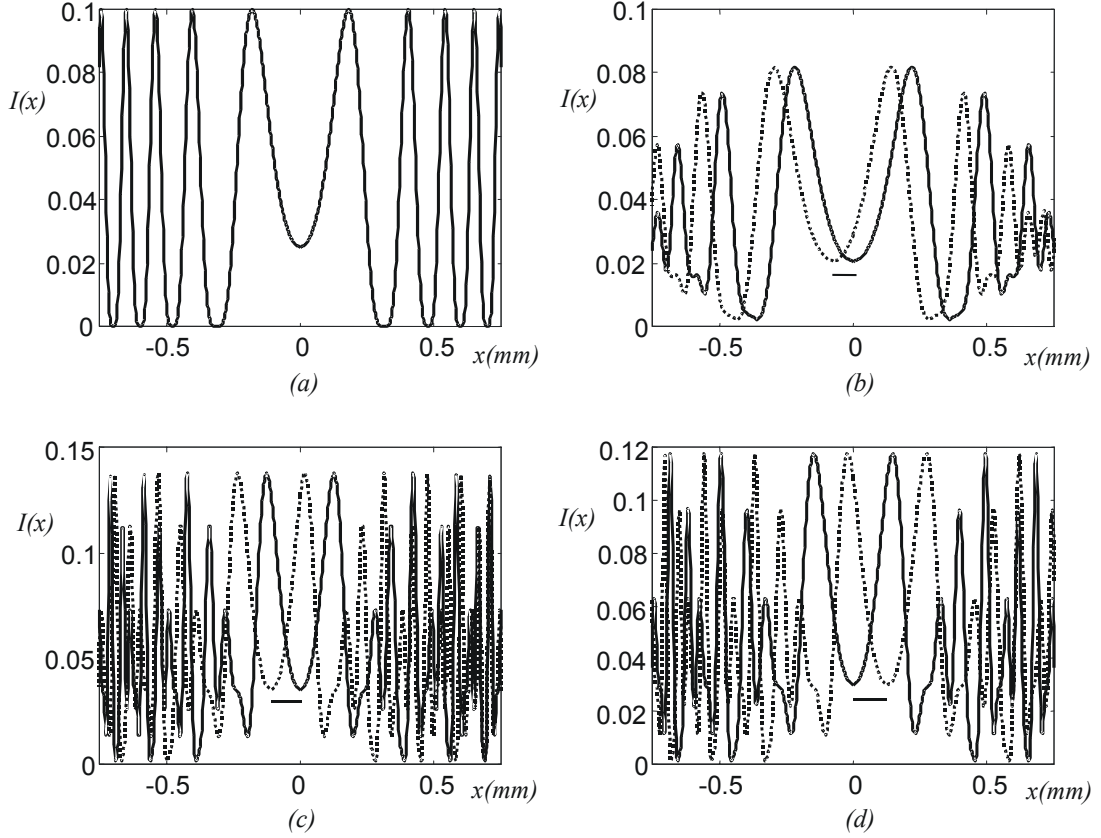


Figure 5: Irradiance distribution for on-axis (solid line) and off-axis (dot line) illuminations at (a) $z = 0$ (input plane), (b) $z = 8.50$ mm, (c) $z = 17.01$ mm (1st. Fourier plane) and (d) $z = 60.20$ mm (2nd. Fourier plane). Calculations have been made for zone plate period $p = 91 \times 10^{-4} \text{ mm}^2$; illumination parameters $\lambda = 1.3 \mu\text{m}$, $d = 10$ mm and $\zeta = 0.15$ mm; and GRIN parameters $n_0 = 1.5$, $g_0 = 0.1 \text{ mm}^{-1}$ and $L = 100$ mm.

4 Influence of finite dimension

Let us now consider a hybrid system of finite dimensions with aperture $2b$ illuminated by an on-axis uniform source located at a distance d from the input face of the structure. In this case, the complex amplitude distribution in the tapered GRIN medium at $z > 0$ becomes

$$\phi(x; z) = \int_{-b_{\text{eff}}}^{b_{\text{eff}}} \phi(x_0) K(x, x_0; z) dx_0, \quad (28)$$

where b_{eff} represents the effective semiaperture [7], related to the semiaperture b as

$$b_{\text{eff}} = n_0 d \left[\frac{g_0 g(z)}{1 + n_0^2 g_0^2 d^2} \right]^{1/2} b \quad (29)$$

and evaluated at the first z plane verifying

$$\tan \left[\int_0^z g(z') dz' \right] = \frac{1}{n_0 g_0 d}. \quad (30)$$

It means that not all the rays reaching the GRIN medium will be confined through it and then there is a spatial limitation in the size of the zone plate. For an explicit derivation of equations (29) and (30), see appendix A.

Substituting equations (2)-(4) and equation (6) into equation (28) and integrating, we arrive at the following complex amplitude distribution

$$\phi(x; z) = \frac{1}{(i2d)^{1/2}} \exp \{ ik(n_0 z + d) \} \sum_{m=-\infty}^{\infty} a'_m(z) \exp \left\{ i \frac{\pi}{\lambda} U_m(z) x^2 \right\} Q_m(x; z), \quad (31)$$

where

$$Q_m(x; z) = Q[\theta_m^+(x; z)] - Q[\theta_m^-(x; z)] \quad (32)$$

and Q is the complex Fresnel integral defined as

$$Q(\tau) = C(\tau) + iS(\tau) = \int_0^\tau \exp \left(i \frac{\pi}{2} t^2 \right) dt, \quad (33)$$

C and S being the real and imaginary parts of Q and

$$\theta_m^\pm(x; z) = \left(\frac{2n_0}{\lambda |H_1(z)| |F_m(z)|} \right)^{1/2} (\pm |F_m(z)| b_{\text{eff}} - x). \quad (34)$$

From equation (31) we arrive at the following expression for the irradiance

$$I(x; z) = \frac{1}{2d} \sum_{m,l=-\infty}^{\infty} a'_m(z) a_l'^*(z) \exp \left\{ i \frac{\pi}{\lambda} [U_m(z) - U_l(z)] x^2 \right\} Q_m(x; z) Q_l^*(x; z), \quad (35)$$

which can be rewritten for the particular hybrid structure discussed in section 2 as

$$\begin{aligned}
 I_s^a(x; z) = & \left\{ \frac{1}{8d} \frac{|Q_o(x; z)|^2}{|F(z)|} + \frac{\varepsilon^2}{4} \frac{|Q_1(x; z)|^2}{|F_1(z)|} + \frac{\varepsilon^2}{4} \frac{|Q_{-1}(x; z)|^2}{|F_{-1}(z)|} \right. \\
 & + \frac{\varepsilon}{|F^{1/2}(z)F_1^{1/2}(z)|} [(\operatorname{Re}[Q_o(x; z)] \operatorname{Re}[Q_1(x; z)] + \operatorname{Im}[Q_o(x; z)] \operatorname{Im}[Q_1(x; z)]) \\
 & \times \sin\left(\frac{\pi}{\lambda}[U(z) - U_1(z)]x^2\right) - (\operatorname{Re}[Q_o(x; z)] \operatorname{Im}[Q_1(x; z)] \\
 & - \operatorname{Im}[Q_o(x; z)] \operatorname{Re}[Q_1(x; z)]) \cos\left(\frac{\pi}{\lambda}[U(z) - U_1(z)]x^2\right)] \\
 & - \frac{\varepsilon}{|F^{1/2}(z)F_{-1}^{1/2}(z)|} [(\operatorname{Re}[Q_o(x; z)] \operatorname{Re}[Q_{-1}(x; z)] + \operatorname{Im}[Q_o(x; z)] \\
 & \times \operatorname{Im}[Q_{-1}(x; z)]) \sin\left(\frac{\pi}{\lambda}[U(z) - U_{-1}(z)]x^2\right) - (\operatorname{Re}[Q_o(x; z)] \operatorname{Im}[Q_{-1}(x; z)] \\
 & - \operatorname{Im}[Q_o(x; z)] \operatorname{Re}[Q_{-1}(x; z)]) \cos\left(\frac{\pi}{\lambda}[U(z) - U_{-1}(z)]x^2\right)] \\
 & - \frac{\varepsilon^2}{2|F_1^{1/2}(z)F_{-1}^{1/2}(z)|} [(\operatorname{Re}[Q_1(x; z)] \operatorname{Re}[Q_{-1}(x; z)] + \operatorname{Im}[Q_1(x; z)] \\
 & \times \operatorname{Im}[Q_{-1}(x; z)]) \cos\left(\frac{\pi}{\lambda}[U_1(z) - U_{-1}(z)]x^2\right) + (\operatorname{Re}[Q_1(x; z)] \operatorname{Im}[Q_{-1}(x; z)] \\
 & - \operatorname{Im}[Q_1(x; z)] \operatorname{Re}[Q_{-1}(x; z)]) \sin\left(\frac{\pi}{\lambda}[U_1(z) - U_{-1}(z)]x^2\right)] \left. \right\}. \quad (36)
 \end{aligned}$$

This expression cannot be applied to image planes since H_1 cancels and the Fresnel integrals behave as if the hybrid system dimensions were unlimited. To find an appropriate expression to evaluate these planes we take into account the Lagrange invariant[8]

$$\dot{H}_1(z)H_2(z) - H_1(z)\dot{H}_2(z) = 1 \quad (37)$$

and use it in equation (9), establishing previously the integral limits from $-b_{\text{eff}}$ to b_{eff} . Making $H_1(z)$ tend to zero we can arrive at the equation

$$\begin{aligned}
 \phi(x; z_q) = & \frac{\exp\{ik(n_0z_q + d)\}}{(H_2(z_q)d)^{1/2}} \\
 & \times \sum_{m=-\infty}^{\infty} a_m \int_{-b_{\text{eff}}}^{b_{\text{eff}}} \exp\left\{i\frac{\pi}{\lambda}\left(\frac{1}{d} - \frac{2m\lambda}{p}\right)x_0^2\right\} \delta\left(x_0 - \frac{x}{H_2(z_q)}\right) dx_0, \quad (38)
 \end{aligned}$$

whose solution is

$$\phi(x; z_q) = \begin{cases} 0, & \text{for } |x| > b_{\text{eff}}, \\ \frac{\exp\{ik(n_0z_q - d)\}}{[H_2(z_q)d]^{1/2}} \exp\left\{i\frac{\pi}{\lambda}\frac{x^2}{dH_2^2(z_q)}\right\} \sum_{m=-\infty}^{\infty} a_m \exp\left\{-i\frac{2\pi m}{p(z_q)}x^2\right\}, & \text{otherwise.} \end{cases} \quad (39)$$

This equation shows that the irradiance at a plane verifying the imaging condition is a replica of the irradiance on the zone plate, and suffers no diffraction, contrary to what happens at the other planes.

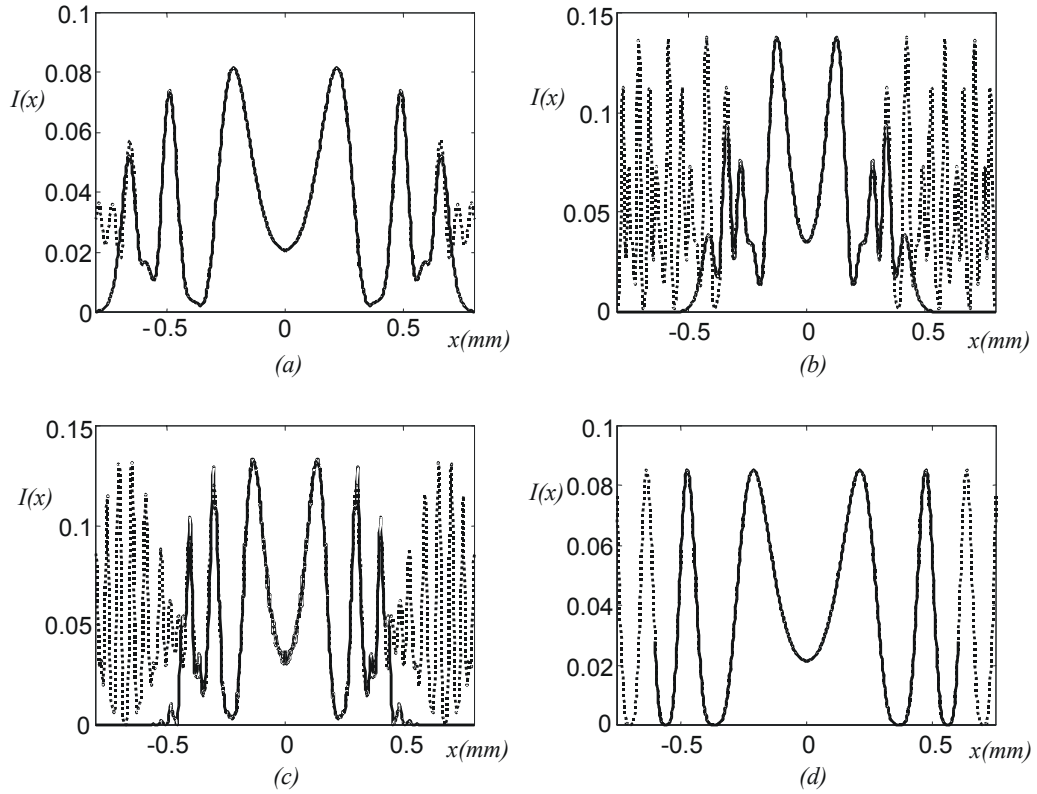


Figure 6: Irradiance distribution at planes (a) $z = 8.50$ mm, (b) $z = 17.01$ mm (1st. Fourier plane), (c) $z = 31.47$ mm and (d) $z = 36.91$ mm (1st. image plane) for a hybrid system of finite transverse dimensions. Calculations have been made for the parameters of figure 5 and an effective aperture $2b_{\text{eff}} = 1.2$ mm. The dotted curves denote the irradiance without the effects of the aperture size.

We can write equation (39) as

$$\begin{aligned} \phi_s^a(x; z_q)|_{|x| < b_{\text{eff}}} &= \frac{\exp\{ik(n_0 z_q + d)\}}{[H_2(z_q)d]^{1/2}} \exp\left\{i\frac{\pi}{\lambda} \frac{x^2}{dH_2^2(z_q)}\right\} \left\{ \frac{1}{2} + \frac{\varepsilon}{4i} \exp\left[i\frac{2\pi x^2}{pH_2^2(z_q)}\right] \right. \\ &\quad \left. - \frac{\varepsilon}{4i} \exp\left[-i\frac{2\pi x^2}{pH_2^2(z_q)}\right] \right\}, \end{aligned} \quad (40)$$

where (16) has been used.

The corresponding irradiance is

$$I_s^a(x; z_q)|_{|x| < b_{\text{eff}}} = \frac{1}{2d|H_2(z_q)|} \left[\frac{1}{2} + \varepsilon \sin\left(\frac{2\pi x^2}{p(z_q)}\right) + \frac{\varepsilon^2}{2} \sin^2\left(\frac{2\pi x^2}{p(z_q)}\right) \right], \quad (41)$$

which is the same as equation (21) but limited to the range $[-b_{\text{eff}}, b_{\text{eff}}]$.

Figure 6 depicts the effects on the irradiance distribution at several planes inside the GRIN medium which arise as a result of the finite dimension of the hybrid system. For comparison, the solid line indicates the irradiance for the case of finite dimension, whereas the dotted line is referred to infinite dimension. Diffraction around the edge of geometrical shadow ($x(z) = b_{\text{eff}}F(z)$) of the periodic object is observed. This edge of geometrical shadow is obtained for (a) $x = 0.73$ mm, (b) $x = 0.43$ mm and (c) $x = 0.45$ mm. In case (d) no diffraction occurs.

5 Summary

The effects of off-axis illumination and finite object dimension on the irradiance distribution in a hybrid system formed by a zone plate and a tapered GRIN medium have been derived and applied to a GRIN medium with a divergent linear taper function and a sinusoidal zone plate of the amplitude. On the one hand, off-axis illumination provides a lateral shift of the irradiance that is centred along a geometrical trajectory proportional to the axial ray and, on the other hand, finite dimension produces in the GRIN medium diffraction around the edge of geometrical shadow of the zone plate. These effects should be taken into account when potential applications in some fields are studied.

Acknowledgment

This work has been supported by the Ministerio de Educación y Cultura, Spain, under contract TIC99-0489.

Appendix A

In a GRIN planar medium of semi-aperture b and length d' illuminated by an on-axis source, a ray will be confined if its height satisfies the condition

$$x(z) \leq b \quad \text{for} \quad 0 \leq z \leq d'. \quad (\text{A.1})$$

Equation (A.1) for the marginal ray becomes

$$x_m = b_{\text{eff}} \left[\frac{H_1(z)}{n_0 d} + H_2(z) \right], \quad (\text{A.2})$$

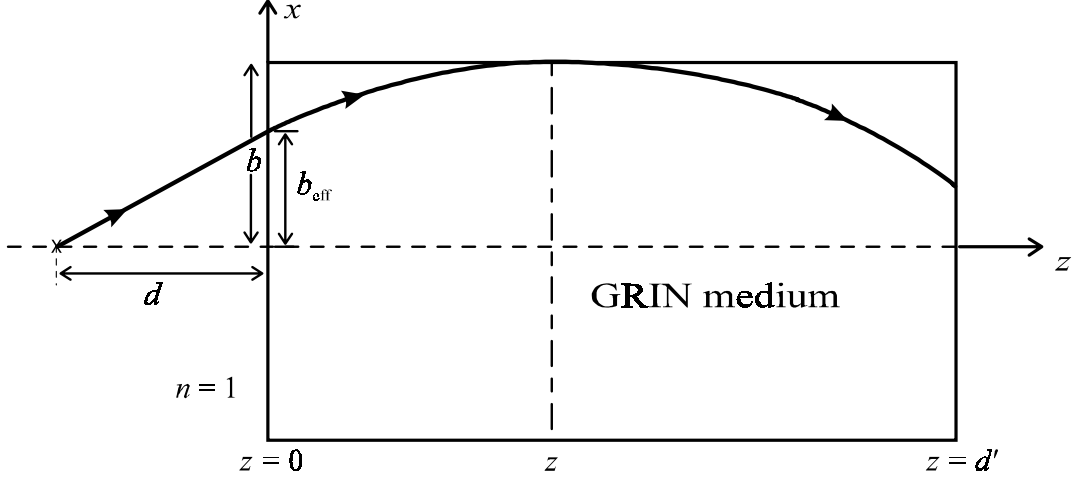


Figure 7: Paraxial marginal ray path in a GRIN medium of semiaperture b for an on-axis point source at a distance d from the input face. b_{eff} is the height of the marginal ray on the input and z the position inside the GRIN medium at which its slope cancels.

where b_{eff} is the incident height of the marginal ray on the input face of the GRIN medium and $b_{\text{eff}}/(n_0 d)$ is the slope of the refracted marginal ray at the input face (figure 7).

Likewise, the slope of the marginal ray at z vanishes, that is

$$0 = b_{\text{eff}} \left[\frac{\dot{H}_1(z)}{n_0 d} + \dot{H}_2(z) \right]. \quad (\text{A.3})$$

From equation (A.3) it follows that

$$\tan \left[\int_0^z g(z') dz' \right] = \frac{1}{n_0 g_0 d}, \quad (\text{A.4})$$

where equations (7-8) have been used.

Substitution of equations (A.4) and (7-8) into equation (A.2) provides

$$b_{\text{eff}} = n_0 d \left[\frac{g_0 g(z)}{1 + n_0^2 g_0^2 d^2} \right]^{1/2} b. \quad (\text{A.5})$$

References

- [1] RIVAS-MOSCOSO, J.M., and GÓMEZ-REINO, C., BAO, C., and PÉREZ, M. V., 2000, *J. Mod. Optics*, **9**, 1549.
- [2] HUNSPERGER, R.G., 1995, *Integrated Optics* (Berlin: Springer-Verlag).
- [3] NIEMEIER, TH. and ULRICH, R., 1986, *Optics Lett.*, **11**, 677.
- [4] YEH, W.-H., MANSURIPUR, M., FALLAHI, M., SCOTT PENNER, R., 1999, *Optics Commun.*, **170**, 207.
- [5] SODHA, M. S., and GHATAK, A. K., 1977, *Inhomogeneous Optical Waveguides* (New York: Plenum Press).
- [6] OJEDA-CASTAÑEDA, J., and GÓMEZ-REINO, C. (eds), 1996, *SPIE Mileston Series*, Vol. MS 128, *Selected Papers on Zone Plates* (Bellingham: SPIE Optical Engineering Press), and references therein.
- [7] HARRIGAN, M.E., 1984, *Appl. Optics*, **16**, 2702.
- [8] GÓMEZ-REINO, C., 1992, *Int. J. Optoelectron.*, **7**, 607.

Figure Captions

- Figure 1. Geometry for the evaluation of the complex amplitude distribution in a hybrid optical system, tapered GRIN medium/zone plate, illuminated by a cylindrical uniform wavefront. Parameter d represents the distance from the point source to the zone plate.
- Figure 2. Equi-index lines for a divergent linear tapered GRIN medium.
- Figure 3. Transmission function of a sinusoidal zone plate of amplitude.
- Figure 4. Geometrical trajectory described by the centre of irradiance pattern. Trajectory amplitude is increasing due to divergent linear taper function.
- Figure 5. Irradiance distribution for on-axis (solid line) and off-axis (dot line) illuminations at (a) $z = 0$ (input plane), (b) $z = 8.50$ mm, (c) $z = 17.01$ mm (1st. Fourier plane) and (d) $z = 60.20$ mm (2nd. Fourier plane). Calculations have been made for zone plate period $p = 91 \times 10^{-4}$ mm²; illumination parameters $\lambda = 1.3$ μ m, $d = 10$ mm and $\zeta = 0.15$ mm; and GRIN parameters $n_0 = 1.5$, $g_0 = 0.1$ mm⁻¹ and $L = 100$ mm.
- Figure 6. Irradiance distribution at planes (a) $z = 8.50$ mm, (b) $z = 17.01$ mm (1st. Fourier plane), (c) $z = 31.47$ mm and (d) $z = 36.91$ mm (1st. image plane) for a hybrid system of finite transverse dimensions. Calculations have been made for the parameters of figure 5 and an effective aperture $2b_{\text{eff}} = 1.2$ mm. The dotted curves denote the irradiance without the effects of the aperture size.
- Figure 7. Paraxial marginal ray path in a GRIN medium of semiaperture b for an on-axis point source at a distance d from the input face. b_{eff} is the height of the marginal ray on the input and z the position inside the GRIN medium at which its slope cancels.